Non-bonded force field for the interaction between metals and organic molecules: A case study of olefins on aluminum

Ling-Ti Kong *, Colin Denniston †, and Martin H.Müser‡
Department of Applied Mathematics, University of Western Ontario
London, Ontario, Canada N6A 5B7

Yue Qi§
Materials and Processes Laboratory, General Motors R&D Center
Warren, MI 48090-9055

April 3, 2009

Abstract

An approach to parameterize the non-bonded force field for the interaction between organic molecules and metal surfaces is suggested. Special attention is paid to the suitability of the resulting potential for tribological situations. As an example, we study olefin molecules residing on aluminum surfaces within the framework of the OPLS force field. Our iterative scheme consists of the following steps: A medium-scale molecular dynamics simulations of olefins confined between two aluminum solids is run under tribological conditions (normal pressure of 0.2 GPa and nominal shear rate of 0.5 GHz) using a guess for the interaction potential. After reaching a local equilibration, molecules near the metal surfaces are isolated and the forces between them and aluminum atoms are computed using density functional theory. The force field parameters are then fit to these forces so that an improved guess for the classical force field is obtained. The steps are repeated until convergence is achieved. In our simulated annealing fits the lateral forces receive a particularly large weight because the corrugation potential is crucial for tribological properties. While our training set only contains hexene molecules, we find that the standard error in the fitted olefin-aluminum interaction increases only by a factor of 1.15 when the force field is applied to butene, octene, and decene. Including mirror charges into the treatment improves fits only marginally. While olefins on aluminum are merely a special case, the proposed methodology can be used to parameterize any other interaction between polymers and metal surfaces for use in tribological simulations.

1 Introduction

The study of interfaces between organic molecules and metal surfaces is of paramount importance to the understanding of many technologically relevant applications. In particular, adsorption[1–3] and diffusion[1,4,5] of oligomers and polymers on metal surfaces is critical in the context of friction and lubrication[6,7] and when organic films form on metal electrodes.[8,9] In order to model interfaces between organic molecules and metals with atomistic principles, i.e., with molecular dynamics (MD), it would be desirable to have reliable force

*Email: lkong7@uwo.ca
†Email: cdennist@uwo.ca
‡Email: mmuser@uwo.ca
§Email: yue.qi@gm.com

fields, because the large diffusive time scales in those systems make first-principle studies generally unfeasible. Such MD simulations would however require a sufficiently accurate classical force field for all involved interatomic forces in order to be meaningful. Similarly, boundary conditions for continuum simulations capable of reaching much longer length and time scales could be derived from atomistic simulations,[10,11] but these will only be as good as the force fields used in the atomistic simulations.

During the past few decades, accurate force fields (FF) for organic molecules[12–15] and also for metals[16] have been developed. Unfortunately, similarly realistic descriptions for the non-bonded interactions between organic molecules and metal atoms are not generally available, despite some progress: For example, Shaffer *et al.* have proposed an orientation dependent functional for the interaction between poly(methyl methacrylate) and aluminum atoms.[17] Fartaria *et al.* have derived a united atom model based on density functional theory (DFT) calculations for the simulating of ethanol adsorption on Au(111) surfaces.[18] Zerbetto and collaborators have adopted an atomic based empirical FF to describe the interaction between alkane and Au(111) surfaces.[19,20] Recently, Zhao *et al.* proposed a semi-ionic model for metal oxides and their interfaces with organic molecules.[21] Nonetheless, these approaches lack either an atomic nature, or a systematic way in determining the necessary FF parameters. More importantly, none of them emphasized the special role of the corrugation potential, whose knowledge is critical when studying diffusion or slip boundary conditions or other tribological properties of the system.[22–24]

In this paper, an iterative scheme is proposed to parameterize non-bonded force fields (NBFF) between metal surfaces and adsorbed polymers. The goal is to overcome the lack of a systematic fitting procedure and to identify suitable functional forms for the interatomic interactions. Special attention is paid to matching (the NBFF and DFT) forces lateral as well as normal to the metal substrate. Correct lateral forces, responsible for the corrugation potential, are crucial when determining dynamic quantities such as the diffusion coefficient or slip boundary conditions.[22,24] Our approach is iterative and similar in spirit to previous fitting schemes:[25–29] Classical MD simulations are run to produce typical configurations, for which forces are calculated with DFT so that the FF can be further improved. Here we extend these ideas to develop NBFF for systems under non-equilibrium conditions. Specifically, we will study the interaction between olefins sheared between aluminum walls within the framework of the OPLS force field.[15] The interest in these materials is motivated by our desire to better understand lubrication of lightweight and thus fuel-efficient, aluminum-based engines.[30]

The remaining content of this paper is organized as follows: in Section 2 the FF forms, the employed DFT, and MD methods, and the fitting procedure are described. The fitting results and the examination of the transferability of the derived force field are presented in Section 3. Finally, a conclusion is drawn in Section 4.

2 Methodology

2.1 Force fields

The purpose of this work is to develop FFs for the interactions between closed-shell hydrocarbons and metal surfaces/atoms. In order to isolate the hydrocarbon-metal interaction, it is necessary to distinguish the intra- and intermolecular as well as intra-metallic forces from the net force that one computes. This way, the parameterization for the intermolecular forces can be done with respect to already existing FFs for intra-molecular and intra-metallic forces.

In the practical use of the FFs developed, we would envision interactions between metal atoms to be described with the embedded atom method (EAM), which has a parameterization for Al available.[31] In the present work, the aluminum walls will be kept rigid so that the Al-Al forces do not enter the MD calculations. The reasons behind keeping the Al rigid were two-fold. First, the Al-Al binding energy is sufficiently strong that rigidity is not a bad approximation. Second, this allows us to represent each aluminum wall by two (111) layers, thus dramatically decreasing the computational cost in the DFT calculations. Interactions between aluminum and olefins decay sufficiently fast for this to be an adequately large number of layers. (DFT calculations of a single 1-butene molecule on two to four Al-layers were used to confirm this assumption.)

Two layers would not be enough, however, to use the EAM to accurately match to DFT for the Al-Al forces (which would typically require more than 4 layers). In this work, we will not discriminate between atoms in the last, second-last, third-last, etc. layer. Thus only one type of aluminum atom will be considered.

In contrast to the aluminum surface, the olefin molecules are quite flexible and molecules cannot be considered to be rigid. For the interactions within and between the olefins, we use the OPLS FF,[14,15] which expresses the potential energy of a system as

$$E = E_{\text{bond}} + E_{\text{angle}} + E_{\text{torsion}} + E_{\text{non-bonded}}, \tag{1}$$

where the first three terms account for the bonding contribution. The non-bonded term consists of a long range Coulombic part due to charges and a pair interaction part. Simple olefin molecules are formed by carbon atoms and hydrogen atoms, with one or more carbon-carbon double bonds in the chain. In the OPLS FF, the carbon atoms are therefore classified into two types according to their bonding nature or hybridization state. A similar classification is applied to the associated hydrogen atoms, specifically, sp^3 carbon is called CT, while sp^2 carbon is denoted by CM. Likewise, one distinguishes between the hydrogen atoms as HT (H attached to CT) and HC (H attached to CM).

Since we restrict our attention to the non-bonded interaction of metal atoms with closed electron-shell molecules, only two-body potentials were investigated for the metal-olefin interaction. Three different short-range pair interaction formulas were tried, namely the Lennard-Jones,[32] the Buckingham[33] and the Morse[34] potential, among which the Buckingham type was found to give the best fit in our preliminary fits. Specifically, the standard error in the force matching (difference between DFT and MD, as defined in the next section) for Lennard Jones was $\sim 50\%$ larger and that for Morse was $\sim 25\%$ larger than that for Buckingham. The Buckingham formula was therefore adopted to describe all these pair interactions:

$$E = A \cdot \exp\left(\frac{-r}{\rho}\right) - \frac{C}{r^6}. \tag{2}$$

In accord with the previous discussion, we will have to parameterize four types of interactions: Al-CT, Al-CM, Al-HT, and Al-HC. Note that the Buckingham potential has a "pathological" singularity at small distances, which will be discussed in more detail in Section 3.

We also investigated the necessity of including long-range electrostatic wall-olefin interactions through the use of mirror charges. As hydrogen and carbon have very similar electronegativity, there is little charge flow between those two atoms resulting in typical charges of roughly 0.1 e in OPLS. Mirror charges induced by these small charges result in forces small compared to those obtained when a molecular film is squeezed with 0.2 GPa against the walls. Typically, the normal force on individual atoms close to the surface would change by less than 1% of the net force. The relative effect is even smaller on grouped or "correlated" units (CH_n units), because each hydrocarbon group is electrically neutral in OPLS. The Coulombic part of the interaction between olefin atoms and the metal atoms is therefore neglected and our interaction is assumed to have a short-range pair part only. However, if highly polar groups were present with atomic charges on the order of 1 e, one may have to include the Coulomb interaction.

2.2 Details of MD and DFT calculations

All classical simulations and the evaluation of MD forces during the fitting procedure were carried out by using the Large-scale Atomic/Molecular Massively Parallel Simulator (LAMMPS).[35–37] Details of the MD simulations, such as the one depicted in the leftmost box of the flowchart in Fig. 1, can be summarized as follows: As mentioned above, the Al walls consisted of two (111) Al layers. The initial size of the simulation cell, which contained 200 1-hexene molecules, was $19.8 \times 20 \times 100$ Å^3 in x, y, and z direction respectively. Periodic boundary conditions were employed in the xy-plane and the cell dimensions of that plane were kept fixed. In the normal direction (z), a pressure of 0.2 GPa was applied to the aluminum walls. This compressive pressure was sufficient to sample the repulsive tails of the interaction between olefins and aluminum. This constant pressure constraint naturally leads to small variations in the normal direction around the initial sample geometry. The top aluminum wall moves at a constant velocity in the x-direction of $v_x = 5$ m/s

while the bottom wall is fixed, resulting in a nominal shear rate of ≈ 0.5 GHz. Atoms were thermostatted at a temperature of 300 K with a Langevin thermostat that acted only normal to the shear plane (i.e. in the y-direction). The time constant associated with the Langevin thermostat was set to 10 ps. Time steps were 1.5 fs and typical runs (starting from previous locally equilibrated configurations) were 6.25 ns.

The DFT calculations of the training configurations as well as the test configurations were performed by using the local-spin-density approximation and generalized gradient corrected exchange and correlation functional PBE.[38] Training and test configurations contained one aluminum wall and one molecule close to that wall. Computations were done by using the plane-wave based Quantum-ESPRESSO package[39] and ultrasoft Vanderbilt pseudopotentials,[40] with a plane wave cutoff of 400 eV. The simulation cell is set to be $\sim 19.8 \times 20 \times 100$ Å^3 in all cases except for single molecules in a large vacuum box used to compare our fitting errors to those of OPLS. Some preliminary work was done using an Aluminum flake (finite in x and y directions, but with more layers normal to the Al-olefin "interface") using the GAUSSIAN package, which is better optimized for atom clusters than periodic systems due to the basis set choice (non-periodic). However, the metal flake had very significant edge effects leading to charge localization (of order ± 1 e) in the metal. This resulted in poorer fits and poorer transferability. As a result, all results reported here are for the systems in which the metal surface was periodic and DFT with the plane-wave basis sets were used.

2.3 Fitting procedure

As described in the introduction, we used an iterative or self-consistent scheme to produce typical and relevant configurations of olefins relative to an aluminum wall. The approach is illustrated in Fig. 1 and can be summarized as follows:

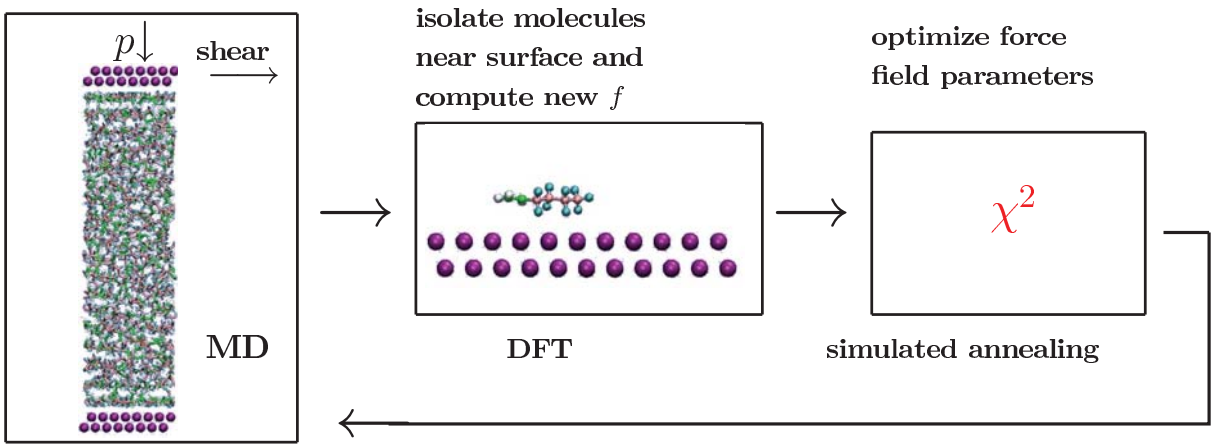

Figure 1: (color online) Illustration of the flow-chart employed for the force field fitting.

1. Run a tribological MD simulation of olefins confined between two aluminum walls using a guess for the olefin-aluminum interaction. See Sect. 2.2 for details. Atomic positions used in the next step are based on the last configuration.
2. Compute the forces, using DFT, from the walls on the molecules selected in step 1.
3. Fit the adjustable parameters of the NBFF to minimize the χ^2 based on the difference between DFT and FF forces.
4. Return to step one with the new set of parameters and repeat until convergence is achieved.

We will now comment in more detail on different aspects of the various steps in our approach. The first choice necessary is what olefin to use in this procedure. The success of OPLS suggests that the force fields

derived for one olefin should transfer to those of another, perhaps longer chain, olefin. The DFT calculations are computationally expensive so one is tempted to minimize this work by using very simple molecules such as methane and ethene for the fits. We initially followed this path, but found that the potentials obtained do not transfer to longer chains (such as octene and decene) as well as we would have liked. As a result, we took the opposite approach and used the longest chain olefin with which both DFT and MD calculations were feasible with limited computer resources, which in this case was hexene. As discussed below, this gives excellent transferability, to longer chains. The poorer transferability of fits done with small molecules is likely to come from a number of sources. One factor is that the carbon atoms in the shorter molecules are always end groups and, due to their attached hydrogen, are kept further from the substrate than, say carbon molecules in the middle of a longer flexible chain with fewer attached hydrogens. Thus the fits are less constrained as the carbons cannot explore close C-Al distances and are biased to marginally better fitting in the repulsive tails, but poorer fitting to closer distances.

The first time one takes step one, it is necessary to start with some initial guess for the force field. Since atomic radii are known as well as rough guesses for the binding energies of non-bonded (meaning non-covalent and non-ionic) interactions, it is not too difficult to make up reasonable numbers for the interaction parameters. At the initial stage, there is no need to distinguish between CT and CM or between HT and HC. To select the DFT configurations for the next step, we take the final molecular dynamics atomic positions and isolate ∼10 molecules near the walls. The CT, CM, HT, and HC atoms that are closest to a wall should be contained in these configurations. In addition, we select some of the 1-hexene molecules and push them even further toward the wall by a rigid translation of 0.5 to 1 Å. This last step is necessary to ensure the fitted potentials are constrained to have physically meaningful behavior at short distances (e.g. a hard-core repulsion). If the shorter range behavior is not sampled in the training set, the fitting procedure may fail to converge (one could end up with a potential that allow olefins to come too close to the surface in the next MD cycle resulting in, say, chemical bonding to the Al surface in the next DFT calculation).

The details of step 3 are crucial in our fitting scheme. When optimizing parameters, it is generally necessary to minimize a suitably-chosen cost function, $\sqrt{\chi^2}$, which in our case is a weighted standard deviation between forces as computed in DFT and those produced by the classical FF (i.e. the fit is a force matching procedure). As discussed in the introduction, we want to have a particularly accurate representation of the corrugation potential. As normal forces tend to exceed lateral forces, it is not appropriate to simply minimize an unweighted standard deviation between DFT and FF forces, but equal emphasis needs to be placed on the lateral components. We achieved this goal with the following definition of χ^2:

$$\chi^2 = \frac{1}{3}\sum_{\alpha}\chi^2_{\alpha}, \tag{3}$$

$$\chi^2_{\alpha} = \frac{\sum_i \left(f^{\mathrm{FF}}_{i\alpha} - f^{\mathrm{DFT}}_{i\alpha}\right)^2}{\sum_i \left(f^{\mathrm{DFT}}_{i\alpha}\right)^2}, \tag{4}$$

where $f^{FF}_{i\alpha}$ is the α Cartesian component of the MD force on the i atom contained in the olefin molecule, and $f^{DFT}_{i\alpha}$ is the corresponding force calculated from DFT. With this definition of χ^2, the relative accuracy of lateral forces is similar to that of the much larger normal forces. Note that the $f^{\mathrm{FF}}_{i\alpha}$ in Eq. (4) contain the already existing OPLS FF contribution due to the intra-molecular interaction of the olefin in addition to the (new) non-bonded interactions. Thus, we cannot expect our fits to be (substantially) better than that of the OPLS FF. Also, when using a different force field (other than OPLS), parameters for the Al-olefin interactions might change slightly.

The fitting in step three is done using a simulated annealing (SA) algorithm.[41] Three independent SA runs were performed each time, by adopting different temperature schemes and random number seeds. This yields three different sets of parameters, whose standard deviations constitute some measure of the uncertainty in the parameters. Once the FF parameters change only within this standard deviation from one iteration to the next, we consider the iterative scheme to be converged.

In order to quantify the performance of the force field, another parameter besides the χ^2 is defined, namely the root-mean-square-difference (RMSD) in forces:

$$\Delta f = \sqrt{\frac{1}{3}\sum_{\alpha} \Delta f_{\alpha}^2}, \tag{5}$$

$$\Delta f_{\alpha} = \sqrt{\sum_{i} \left(f_{i\alpha}^{\mathrm{FF}} - f_{i\alpha}^{\mathrm{DFT}}\right)^2}, \tag{6}$$

where α numerates the Cartesian component and i goes over all atoms. For an acceptable set of parameters, we would expect that the resultant χ^2 and/or Δf share a similar value with those of OPLS for isolated olefin molecules.

3 Results

3.1 Parameters and validation of the fitted NBFF

Following the scheme outlined in the last section, four iterations were required to reach our stop criterion. Results are summarized in Table 1 for the last round of fitting. The non-bonded FF parameters obtained using three different simulated annealing runs (different temperature schemes, different random number sequences, but the same input data) are listed along with the χ^2's and RMSD Δf's. One can see that the parameters from the three different SA runs are quite close to each other, suggesting that all three parameter sets have converged to the vicinity of the global minimum of the χ^2 for the training configurations.

To ascertain that these parameters are acceptable, the 1-hexene molecules in the training configurations of the last round fitting were put in a large vacuum box and then subjected to both DFT and MD calculations to get the intramolecular forces on each atom (i.e. forces not involving Al). Table 2 lists the χ^2 and RMSD Δf obtained, which measures the agreement between DFT forces and those by the OPLS FF for pure 1-hexene molecules. Comparing the data listed in Tables 1 and 2, one sees that both the χ^2 and Δf of the fitted NBFF are similar in magnitude to those of the the OPLS FF for pure 1-hexene molecules, suggesting that these parameters are acceptable (in the sense that the fits are as good as the underlying OPLS FF). However, one also notices that both χ^2 and Δf of the NBFF are slightly greater than those of the OPLS FF, especially Δf.

To explore the origin of the slightly larger χ^2, recall that in some of the training configurations, the 1-hexene molecules were artificially translated toward the aluminum wall (0.5 to 1 Å). In reality, these would be a very rare event for a molecule to explore. If these configurations are excluded in the evaluation of the RMSD Δf, leaving only training set configurations from what should be a canonical ensemble, its value would be reduced to 9.3395 kcal/(mol·Å), which is even smaller than that of 9.4922 kcal/(mol·Å) by OPLS for pure 1-hexene molecules. It is therefore believed that the derived NBFF parameters will not degrade the performance of the OPLS FF when applied to the study of interactions between 1-hexene and aluminum substrates. The average value of the parameters from the three independent SA runs yields similar χ^2 and Δf, and we therefore adopt the average values as being sufficiently close to the optimal parameters.

The force fields resulting from the optimal parameters are shown in Fig. 2, which displays the potential energies as a function of distance for the four non-bonded pairs parameterized in this work. One notices substantial differences between the Al-CT and the Al-CM potentials, namely the latter has a slightly deeper minimum and the sp^2 carbon 'wants' to approach the Al atoms more closely than the sp^3 carbon. The Al-H interactions have a binding energy of roughly 3 kcal/mol, which one could classify as a weak hydrogen bond.

It is also observed in Fig. 2 that at small distances, there is a crossover in the energy curve, yielding attractive interactions instead of strong repulsive interaction at very small distances. This is an unwanted but generic feature of the Buckingham formula which, however, should not be of any practical relevance unless local pressures or temperature are ridiculously high. The thermal energy barrier that an Al-CM pair initially at a distance of a couple of angstroms would have to cross to get into this attractive well is

Table 1: Comparison of non-bonded force field parameters from three independent simulated annealing runs in the last round of fitting, together with the comparison of forces against the DFT data. A is in unit of kcal/mol, ρ in Å, and C in Å^6·kcal/mol; the χ^2s are unitless, while the RMSD Δf's are in unit of kcal/(mol·Å).

Run ID		1	2	3	Average
Al-CT	A	8731.4	8699.8	8745.3	8725.5± 23.3
	ρ	0.47293	0.47311	0.47285	0.47296±0.00013
	C	5656.5	5640.1	5662.7	5653.1± 11.7
Al-CM	A	25705	25680	25673	25686± 17
	ρ	0.39201	0.39208	0.39209	0.39206±0.00004
	C	8018.1	8018.9	8017.6	8018.2±0.7
Al-HT	A	71703	71743	71764	71737± 31
	ρ	0.20557	0.20557	0.20560	0.20558± 0.00002
	C	461.61	461.97	462.70	462.09±0.56
Al-HC	A	51659	51668	51614	51647± 29
	ρ	0.23081	0.23087	0.23086	0.23085± 0.00003
	C	728.69	730.11	728.99	729.27± 0.75
	χ^2_x	0.1457	0.1457	0.1457	0.1457
	χ^2_y	0.1996	0.1996	0.1996	0.1996
	χ^2_z	0.1249	0.1249	0.1249	0.1249
	χ^2	0.1567	0.1567	0.1567	0.1567
	Δf_x	10.9046	10.9042	10.9044	10.9042
	Δf_y	11.2084	11.2085	11.2081	11.2083
	Δf_z	11.7400	11.7404	11.7407	11.7406
	Δf	11.2896	11.2897	11.2897	11.2897

Table 2: Cost function χ^2 and RMSD for the forces of an isolated 1-hexene molecule.

component	x	y	z	total
χ^2	0.1275	0.1401	0.1804	0.1493
Δf	9.1207	8.0497	11.0598	9.4922

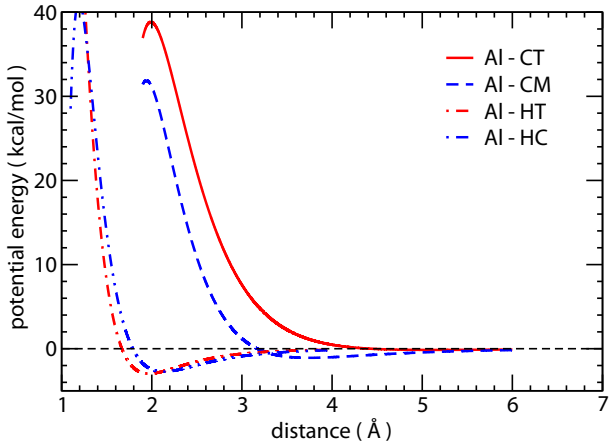

Figure 2: (color online) Potential energies as a function of distance for non-bonded pair interaction between olefin and aluminum atoms from the fitted optimal force field parameters.

$\sim$ 16000 K (i.e. more than 50 times the typical thermal energy of atoms at room temperature). This barrier will be further increased by the hydrogen atoms that are bonded to the carbon atom and that have even higher energy barriers. If a situation arises in an MD simulation, where these barriers are overcome, one can be certain that the interaction potential is not appropriate for these extreme conditions to begin with and a collapse into the singularity may be a 'healthy' warning sign that the outcome of the simulation should not be trusted. One should however be careful to ensure that initial configurations in an MD simulation do not violate this barrier.

3.2 Analysis of correlated units

The final goal of our study is to design a potential to use in the measurement of diffusion constants and slip boundary conditions of polymers on metal surfaces. In this context it is important to realize that the determining factor for these quantities is how "elastically correlated units" feel the corrugation rather than what lateral forces are exerted on individual atoms.[42] (The persistence length would be an upper bound for the linear dimension of an elastically correlated unit.) It is thus an interesting question to ask if errors accumulate or annihilate when certain chemically bonded units (e.g. CH_n groups) are grouped together. To answer this question, the force components are shown in Fig. 3 for individual atoms of the configurations contained in the last training set. One can see that there is the following tendency as far as lateral forces are concerned: If the lateral force of a carbon atom is overestimated in the FF, then the force on its attached hydrogen atoms tend to be underestimated and vice versa. This observation can be interpreted as follows: Whenever a C-H bond sits close to the Al surface but crosses (in xy plane) an Al-Al bond, the C and the H atoms will experience an additional repulsion but, figuratively speaking, the H atom is pushed roughly as much to the left as the C atom is pushed to the right, so that this bond crossing does not result in a net force on that correlated unit.

In order to make this analysis more quantitative, we separated the 1-hexene molecule into three correlated groups: [CH_2=CH], [CH_2], and [CH_3]. The resulting χ^2's are again defined via Eqs. (3) and (4), except that now the index i runs over the groups. The grouped χ^2 turned out to be only 2/3 of the atomic χ^2 so that the potential appears to show favorable properties regarding coarse-grained properties. However, a similar improvement of the forces upon grouping was not observed for longer olefins, which will be discussed in the next section.

One may ask why we did not fit to the grouped forces if our goal is to optimize those. The reason is that such fits have more and broader basins of attraction for the fit parameters. This is due to the fact that the

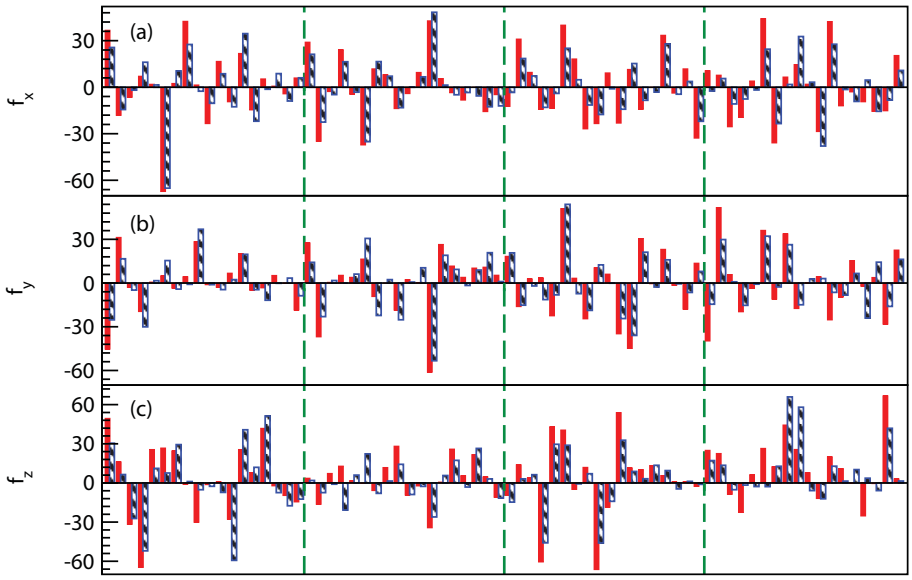

Figure 3: (color online) Comparison of the forces obtained by DFT calculations (red solid bars) and those by the fitted force field (blue broken bars) on each atom in four of the training configurations. (a)–(c) are the x, y, and z component of the forces on each atom of these two configurations, respectively. Forces are in unit of kcal/(mol·Å). Dashed vertical lines separate different configurations. The sequence of the atoms is CH_2=CH-CH_2-CH_2-CH_2-CH_3.

repulsion between aluminum and hydrogen atoms can be shifted to or from the repulsion between aluminum and carbon atoms. As a result, the potentials for the hydrogens resulting from grouped fits tended to have unphysical steep minima and very small values for ρ. For this reason and because the grouped χ^2 turned out reasonably small when adjusting the FF parameters to the atomic χ^2, we abandoned the idea of fitting to grouped forces.

3.3 Transferability of the fitted force field

The non-bonded force field we obtained was based on the training configurations of 1-hexene molecules on aluminum substrates and we have shown that it is capable of reproducing the DFT forces on hexene molecules in a satisfactory way. It is expected that the derived non-bonded FF would work as well in describing the

Table 3: Comparison of forces from the fitted force field to those obtained by DFT calculations for ethene, 1-butene, 1-octene, and 1-decene.

	ethene	1-butene	1-hexene	1-octene	1-decene
χ^2_x	0.5262	0.2692	0.1457	0.1774	0.2322
χ^2_y	0.4420	0.0955	0.1996	0.2972	0.1918
χ^2_z	0.1527	0.1832	0.1249	0.2564	0.2844
χ^2	0.3736	0.1826	0.1567	0.2436	0.2361
Δf_x	13.3252	9.8443	10.9042	8.4430	9.9029
Δf_y	10.7066	6.4969	11.2083	8.2493	6.9275
Δf_z	9.42069	9.9986	11.7406	11.0654	10.4168
Δf	11.2686	8.9273	11.2897	9.3413	9.2117

interaction between other olefin and aluminum atoms. However, this is not guaranteed and it is therefore necessary to examine its transferability when applied to other olefin–aluminum systems. Accordingly, steps 1–2 of the fitting procedure were repeated by replacing the 1-hexene molecules with ethene, 1-butene, 1-octene, and 1-decene molecules, respectively. The previously fitted FF was used to describe the interaction between olefin and aluminum walls. Around 5 olefin molecules in the vicinity of the walls together with the nearby wall atoms were chosen to form the test set for each kind of olefin molecule, which were then subject to DFT calculations. After that, the forces by the fitted NBFF were also calculated and compared to those given by the DFT calculations. Table 3 shows the comparison.

It is seen that when the fitted NBFF is applied to other olefin-aluminum systems, the resultant Δf is on the same level as it was applied to hexene-aluminum systems. The derived χ^2's, however, are found to be somewhat higher than that for hexene. It is clear that the comparable RMS difference in forces supports the argument that the derived NBFF can be transferred to other olefin-aluminum system. One might think that the increase in χ^2 would contradict such a conclusion. However, larger χ^2's do not indicate that the fitted NBFF degrades the performance of the underlying OPLS FF: the 1-decene molecules in the verification configurations were also put in a large vacuum box and then subjected to both DFT and MD simulations to get the forces on each atoms, it is found that the χ^2 between the forces by OPLS FF and those by DFT calculations is 0.2356, which is quite close to the value of 0.2361 by the fitted NBFF. It is therefore believed that the presently derived NBFF will not degrade the performance of the OPLS FF when employed to describe the olefin-aluminum interactions, thus confirming the transferability of the fitted NBFF to other olefin-aluminum systems. As discussed in Section 2.3, the ethene molecule is just two end units which, although slightly different from CH_n units interior to the chain, are not given special designation in OPLS and the slightly larger χ^2 is thus expected here too.

4 Conclusion

In conclusion, a systematic approach to derive the non-bonded force field for describing the interaction between organic molecules and metals based on density functional theory calculations was proposed. The non-bonded force field is designed to work along with the existing full atom force field for organic-organic interactions, OPLS. The proposed approach consists of a recursive procedure, aiming at generating a force field that is compatible to the desired working conditions — in the present case, with an emphasis on contact mechanics applications. The stop criterion of this procedure is designed to reproduce the DFT forces within the same accuracy as the underlying OPLS force field.

By employing the proposed approach, a non-bonded force field for olefin and aluminum interaction was developed, by taking 1-hexene molecules on aluminum surfaces as training sets. The fitted non-bonded force field, together with the existing force field employed to describe interactions other than olefin-aluminum non-bonded interactions, is found to be capable of reproducing the DFT forces for the training configurations as accurately as the existing force field for pure 1-hexene molecules. It is also found that the fitted force field works as well in describing the interaction between longer and shorter olefin molecules and the aluminum surfaces, proving the transferability of the fitted non-bonded force field, as well as the feasibility of the proposed approach of force field fitting.

The parameters for the non-bonded interaction between olefin molecules and aluminum substrates developed here are merely a special case. The fitting procedure employed is expected to be of general interest in parameterizing any other interaction between polymers and metal surfaces especially for tribological applications.

5 Acknowledgments

We are grateful for financial support from NSERC and GM. We would also like to thank Razvan Nistor and Kevin Green for help on first principles calculations and force field fittings.

References

[1] F. Rosei, M. Schunack, Y. Naitoh, P. Jiang, A. Gourdon, E. Laegsgaard, I. Stensgaard, C. Joachim and F. Besenbacher, *Progress in Surface Science*, 2003, **71**, 95–146.

[2] S. M. Barlow and R. Raval, *Surface Science Reports*, 2003, **50**, 201–341.

[3] Y. B. Vysotskii and V. S. Bryantsev, *Theoretical and Experimental Chemistry*, 1999, **35**, 265–269.

[4] R. Otero, F. Hümmelink, F. Sato, S. B. Legoas, P. Thostrup, E. Lægsgaard, I. Stensgaard, D. S. Galvão and F. Besenbacher, *nature materials*, 2004, **3**, 779–782.

[5] D. Mukherji and M. H. Müser, *Physical Review E (Statistical, Nonlinear, and Soft Matter Physics)*, 2006, **74**, 010601.

[6] F. P. Bowden and D. Tabor, *The Friction and Lubrication of Solids*, Oxford University Press, 2nd edn., 1986.

[7] M. H. Müser, M. Urbakh and M. O. Robbins, *Adv. Chem. Phys.*, 2003, **126**, 187–272.

[8] N. Koch, *J. Phys. Condens. Matter*, 2008, **20**, 184008.

[9] F. Rosei, M. Schunach, P. Jiang, A. Gourdon, E. Lægsgaard, I. Stensgaard, C. Joachim and F. Besenbacher, *Science*, 2002, **296**, 328–331.

[10] C. Denniston and M. O. Robbins, *Physical Review Letters*, 2001, **87**, 178302.

[11] C. Denniston and M. Robbins, *J. Chem. Phys.*, 2006, **125**, 214102.

[12] J. Ponder and D. Case, *Adv. Prot. Chem.*, 2003, **66**, 27–85.

[13] A. MacKerel Jr., C. Brooks III, L. Nilsson, B. Roux, Y. Won and M. Karplus, in *CHARMM: The Energy Function and Its Parameterization with an Overview of the Program*, ed. P. v. R. Schleyer et al., John Wiley & Sons: Chichester, 1998, vol. 1, pp. 271–277.

[14] W. L. Jorgensen and J. Tirado-Rives, *J. Am. Chem. Soc.*, 1988, **110**, 1657–1666.

[15] W. L. Jorgensen, D. S. Maxwell and J. Tirado-Rives, *J. Am. Chem. Soc.*, 1996, **118**, 11225–11236.

[16] M. S. Daw and M. I. Baskes, *Phys. Rev. B*, 1984, **29**, 6443.

[17] J. S. Shaffer, A. K. Chakraborty, M. Tirrell, H. T. Davis and J. L. Martins, *The Journal of Chemical Physics*, 1991, **95**, 8616–8630.

[18] R. P. S. Fartaria, F. F. M. Freitas and F. M. S. S. Fernandes, *International Journal of Quantum Chemistry*, 2007, **107**, 2169–2177.

[19] G. Teobaldi and F. Zerbetto, *The Journal of Physical Chemistry C*, 2007, **111**, 13879–13885.

[20] R. J. Baxter, G. Teobaldi and F. Zerbetto, *Langmuir*, 2003, **19**, 7335–7340.

[21] L. Zhao, L. Liu and H. Sun, *The Journal of Physical Chemistry C*, 2007, **111**, 10610–10617.

[22] M. H. Müser, L. Wenning and M. O. Robbins, *Phys. Rev. Lett.*, 2001, **86**, 1295–1298.

[23] D. Mukherji and M. H. Müser, *Macromolecules*, 2007, **40**, 1754–1762.

[24] Q. Zhang, Y. Qi, J. Louis G. Hector, T. Cagin, W. A. Goddard and III, *Physical Review B (Condensed Matter and Materials Physics)*, 2007, **75**, 144114.

[25] P.-O. Norrby and T. Liljefors, *Journal of Computational Chemistry*, 1998, **19**, 1146–1166.

[26] P.-O. Norrby, K. Wärnmark, B. Åkermark and C. Moberg, *Journal of Computational Chemistry*, 1995, **16**, 620–627.

[27] J. R. Maple, M.-J. Hwang, T. P. Stockfisch, U. Dinur, M. Waldman, C. S. Ewig and A. T. Hagler, *Journal of Computational Chemistry*, 1994, **15**, 162–182.

[28] M. J. Hwang, T. P. Stockfisch and A. T. Hagler, *Journal of the American Chemical Society*, 1994, **116**, 2515–2525.

[29] S. Chakravorty and C. H. Reynolds, *Journal of Molecular Graphics and Modelling*, 1999, **17**, 315 – 324.

[30] C. Campañá, M. H. Müser, C. Denniston, Y. Qi and T. A. Perry, *Journal of Applied Physics*, 2007, **102**, 113511.

[31] X.-Y. Liu, F. Ercolessi and J. B. Adams, *Modelling and Simulation in Materials Science and Engineering*, 2004, **12**, 665–670.

[32] J. E. Lennard-Jones, *Proc. Phys. Soc.*, 1931, **43**, 461–482.

[33] R. A. Buckingham, Proceedings of the Royal Society of London. Series A, Mathematical and Physical Sciences, 1938, pp. 264–283.

[34] P. M. Morse, *Phys. Rev.*, 1929, **34**, 57–64.

[35] S. J. Plimpton, *J. Comp. Phys.*, 1995, **117**, 1–19.

[36] S. J. Plimpton, R. Pollock and M. Stevens, Proc of the Eighth SIAM Conference on Parallel Processing for Scientific Computing, Minneapolis, MN, 1997.

[37] Large-scale Atomic/Molecular Massively Parallel Simulator, LAMMPS, available at: http://lammps.sandia.gov.

[38] J. P. Perdew, K. Burke and M. Ernzerhof, *Phys. Rev. Lett.*, 1996, **77**, 3865–3868.

[39] QUANTUM-ESPRESSO is a community project for high-quality quantum-simulation software, based on density-functional theory, and coordinated by Paolo Giannozzi. See http://www.quantum-espresso.org and http://www.pwscf.org.

[40] We used the pseudopotentials Al.pbe-n-van.UPF, C.pbe-van_ak.UPF and H.pbe-van_ak.UPF from the http://www.quantum-espresso.org distribution.

[41] W. L. Goffe, G. D. Ferrier and J. Rogers, *Journal of Econometrics*, 1994, **60**, 65–99.

[42] M. H. Müser, *Europhysics Letters*, 2004, **66**, 97–103.